(2)

SECURITY CLASSIFICATION OF THIS PAGE (When Data Entered)

REPORT DOCUMENTATION PAGE

READ INSTRUCTIONS BEFORE COMPLETING FORM

1. REPORT NUMBER: 15199.9-PH	2. GOVT ACCESSION NO.: N/A (AD-A129653)
3. RECIPIENT'S CATALOG NUMBER: N/A	
4. TITLE (and Subtitle): Computer Molecular Dynamics Simulation Studies of Grain-Boundary Structures. II. Migration, Sliding, and Annihilation in a Two-Dimensional Solid	5. TYPE OF REPORT & PERIOD COVERED: Reprint
	6. PERFORMING ORG. REPORT NUMBER: N/A
7. AUTHOR(s): George H. Bishop, Jr. Sidney Yip; Ralph J. Harrison; Thomas Kwok	8. CONTRACT OR GRANT NUMBER(s): DAAG29 78 C 0006
9. PERFORMING ORGANIZATION NAME AND ADDRESS: Massachusetts Institute of Technology, Cambridge, MA 02139	10. PROGRAM ELEMENT, PROJECT, TASK AREA & WORK UNIT NUMBERS: N/A
11. CONTROLLING OFFICE NAME AND ADDRESS: U. S. Army Research Office, P. O. Box 12211, Research Triangle Park, NC 27709	12. REPORT DATE: Aug 82
	13. NUMBER OF PAGES: 8
14. MONITORING AGENCY NAME & ADDRESS(if different from Controlling Office)	15. SECURITY CLASS. (of this report): Unclassified
	15a. DECLASSIFICATION/DOWNGRADING SCHEDULE

16. DISTRIBUTION STATEMENT (of this Report)

Submitted for announcement only.

DTIC ELECTE JUN 22 1983 S B

17. DISTRIBUTION STATEMENT (of the abstract entered in Block 20, if different from Report)

18. SUPPLEMENTARY NOTES

19. KEY WORDS (Continue on reverse side if necessary and identify by block number)

20. ABSTRACT (Continue on reverse side if necessary and identify by block number)

DD FORM 1 JAN 73 1473 EDITION OF 1 NOV 65 IS OBSOLETE

Unclassified

SECURITY CLASSIFICATION OF THIS PAGE (When Data Entered)

Computer molecular dynamics simulation studies of grain-boundary structures. II. Migration, sliding, and annihilation in a two-dimensional solid

George H. Bishop, Jr. and Ralph J. Harrison
Army Materials and Mechanics Research Center, Watertown, Massachusetts 02172

Thomas Kwok and Sidney Yip
Department of Nuclear Engineering, Massachusetts Institute of Technology, Cambridge, Massachusetts 02139

(Received 22 December 1981; accepted for publication 7 April 1982)

The dynamics of a high-angle tilt boundary in a triangular lattice with a truncated Lennard-Jones potential has been simulated by the method of computer molecular dynamics. Boundary migration was observed at various temperatures above a threshold, and was interpreted in terms of small steps involving coupled sliding and migration. In some cases, the simulation proceeded to the annihilation of a pair of boundaries with the attendant release of the boundary free energy and delocalization of the boundary free volume.

PACS numbers: 61.70.Ng, 66.30.Lw, 62.20.Fe

I. INTRODUCTION

Despite the important role of grain boundaries in materials properties, our knowledge of how boundaries actually move at the microscopic level is limited.[1] Much of the difficulty is due to the lack of a suitable means of observing the dynamical processes with sufficient spatial and time resolution. However, through computer simulation, one can obtain detailed atomistic information about model systems, and depending on the choice of interatomic potential function, it is possible to simulate, to a quite reasonable level of accuracy, structural and dynamic properties of real materials.[2–6] Both static[7] and dynamic[8–11] simulations of grain boundaries have been carried out. In the latter studies, one follows the atomic trajectories by numerically integrating the Newton's equations of motion over a succession of small time intervals for a system consisting of several tens to several hundreds of particles.

In this paper, we present results on computer molecular dynamics simulations of a two-dimensional solid containing two high-angle tilt boundaries. The system was a cell of 56 atoms interacting via a Lennard-Jones 6–12 potential, and periodic border conditions were employed to eliminate surface effects. Initially, the system was relaxed at zero temperature, then it was brought up to equilibrium at various temperatures and the behavior of the grain boundaries monitored by following the atomic positions as a function of time.

The principal result of the study is the observation of the detailed atomic motions involved in grain boundary migration. At sufficiently high temperature the two boundaries in the simulation cell both underwent migration and eventually annihilated to form a single crystal. The migration was found to be thermally activated, since below a certain threshold temperature, no migration occurred in the time interval of simulation.

The present results therefore indicate that atomic motions in a grain boundary are highly cooperative and depend to a considerable extent on the boundary structure. Moreover, they show that migration involves a local shear at the boundary, thus implying that grain boundary migration in real solids occurs by a grain boundary dislocation mechanism. We will also see below that the concept[12] of the DSC (Displacement Shift Complete) lattice is particularly useful in interpreting the computer results.

II. CONSTRUCTION OF SIMULATION CELL

The simulation cell contains all the particles whose trajectories are to be calculated explicitly using the equations of motion. Periodic border conditions have the effect of surrounding the simulation cell with image cells generated by translating the simulation cell along the x and y directions by distances equal to the cell dimensions in the two directions. They eliminate explicit surface effects by ensuring that particles in the simulation cell close to the cell border will see the same environment as if they were in the cell center. Whatever defect structure that is present in the simulation cell is reproduced in the image cells, and the simulation is that of an infinite array of defects. Normally one needs to consider only the immediate neighboring image cells when considering forces on atoms in the simulation cells, but when atoms move more than a small fraction of the cell dimension, it is necessary to include more distant image cells.[13]

The simulation cell is constructed by considering a bicrystal of two identical hexagonal lattices which are rotated with respect to one another as shown in regions A and B of Fig. 1(a). The rotation, in this case 38.21° between close packed directions, is chosen to be a coincidence misorientation; that is, one which brings a certain fraction, $1/\Sigma$, of the lattice sites of the two rotated lattices into geometric coincidence ($\Sigma = 7$). This can be seen in region C where the two crystals interpenetrate. The coincidence sites form a superlattice, the coincidence site lattice (CSL).[14] A coincidence boundary was chosen for study because the boundaries are fundamental to current geometric models for grain boundary structure.[12,15,16] Further, such boundaries have a periodic structure, the periodicity of the CSL giving the periodicity of possible grain boundaries at the coincidence misorientation, consistent with the use of periodic borders on cell faces normal to the boundary plane.

 0021-8979/82/085609-08$02.40

Figure 1(a) also shows in region D a fine rectangular grid delineating the {541} and {321} planes in each crystal. Half the points in this grid also represent points in the DSC lattice.[12] To understand its significance, one should note that a general translational displacement of one of the rotated lattices with respect to the other will disrupt the coincidence pattern and the coincidence sites. However, when this displacement is a DSC lattice vector, the coincidence pattern will be restored, usually with a shift in location of the boundary. In the following, the DSC lattice is repeatedly used as a metric in constructing the computational cell and in describing atom displacements as Fig. 1(a) suggests. More importantly, the lattice plays a fundamental role in the interpretation of the migration behavior observed in the simulation.

The DSC lattice for the $\Sigma = 7$ CSL is also hexagonal with a nearest-neighbor distance 1/7 that of the CSL. Again it is more convenient to use a centered rectangular cell. The unit vectors of that cell are [100] DSC = 1/7 [100] CSL = $(a/14)\langle 321\rangle$, and [010] DSC = 1/7 [010] CSL = $(a/14)\langle 541\rangle$. The detailed relation between the fine grid in Fig. 1(a) and the hexagonal and rectangular DSC unit cells are shown in Figs. 1(b) and 1(c).

Our molecular dynamics simulation was initialized using a statically relaxed cell, with dimensions XL = 7 [100] DSC = CSL in the x direction and $YL = 28.607$ [010] DCS = 4.087 CSL in the y direction. Dimension YL was determined by adjusting the free volume at the boundary, as will be discussed later. The 56-atom simulation cell contains two grain boundaries, the second boundary being a result of the periodic border conditions on the y border; for example, Fig. 1(a) shows the bottom half of the kite structure in the bottom border of the cell. The two boundaries are crystallographically identical but of opposite rotational sense. The atoms in the two boundaries are out of the range of direct interaction through the pair potential; however, the boundaries affect each other slightly through the long-range components of their elastic strain field. Because of the opposite rotational sense, one may expect that if they are moved close enough to each other they will attract since their mutual annihilation would reduce the system potential energy. From the present results it appears that the attraction persists even out to their initial separation distance. Since the boundaries initially form part of an equally spaced infinite array, there must be zero force on any individual boundary from its neighboring boundaries until the symmetry is broken by the motion of a boundary with respect to its nearest neighbors. In the simulation the two boundaries are dynamically independent, in the sense that atom motions at the two boundaries are uncorrelated except for long-time average behavior reflecting the elastic interaction.

The particular YL value above was reached after a static relaxation study to obtain a 0 °K equilibrium structure with the proper free volume V_f at the boundary.[17] Here V_f is the volume occupied by atoms in a box containing a grain boundary in excess over the volume occupied by the same number of atoms in a perfect crystal, the extent of the box in the direction normal to the boundary being somewhat larger than the range of the elastic field of the boundary. In the unrelaxed geometric model of the boundary [Fig. 2(a)], the

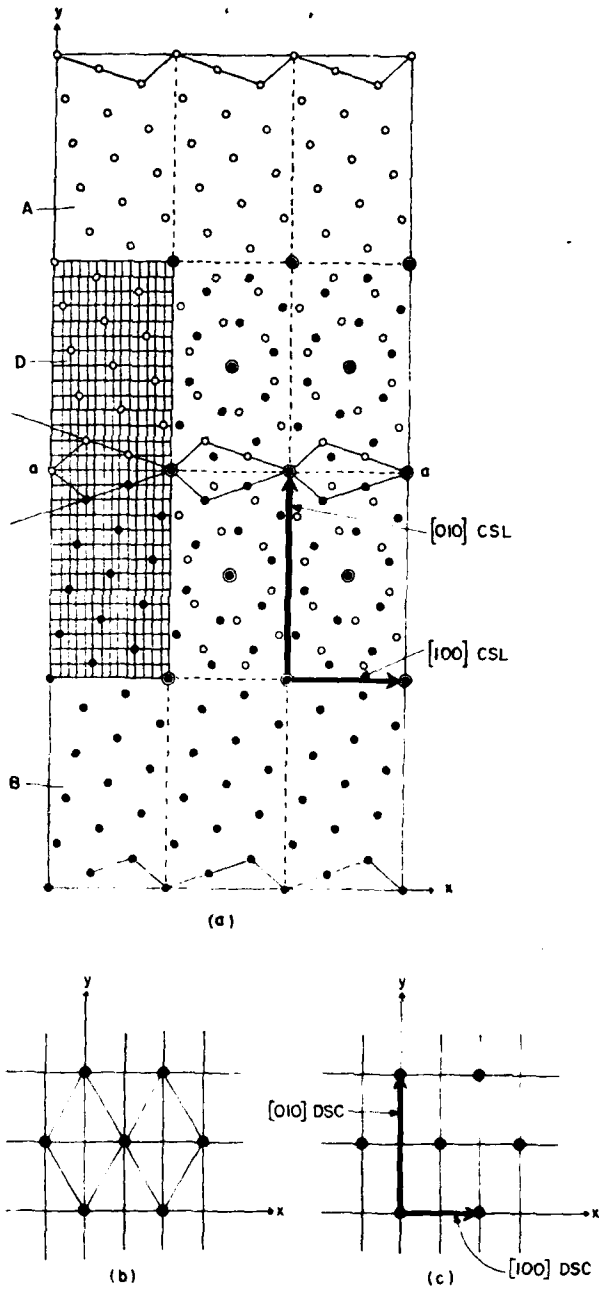

FIG. 1. (a) Construction of a tilt-angle grain boundary in a two dimensional crystal. Regions A and B show the upper and lower halves of a hexagonal bicrystal. Notice the arrays in one region are rotated by an angle of 38.21° with respect to the arrays in the other region. Both arrays are shown in C where several coincidence sites can be seen, with each surrounded by a ring of atoms from either A or B. Throughout this paper, the kite-shaped structure will be used as a pattern recognition aid outlining the arrrangement of atoms at the grain boundary. The boundary itself is located along line a-a. Region D shows a portion of the simulation cell. (b) Hexagonal unit cell of DSC lattice. (c) The face-centered rectangular DSC lattice unit cell defining [100] DSC and [010] DSC.

density of the boundary region is the same as that in a perfect crystal. There is, however, a pair of atoms in each period, adjacent to the kite tail, whose spacing is appreciably less

than the normal nearest-neighbor distance. Such a "tight pair" is a high energy configuration, and during relaxation there will be a local expansion in the boundary region to relax the tight pair. This relaxation will locally decrease the density of the boundary and introduce free volume. Unless the cell is properly adjusted to accommodate the free volume, there will be a uniaxial tensile or compressive strain in the direction normal to the boundary, superimposed on the usual boundary elastic strain field, and extending throughout the cell.

There are several ways of adjusting the simulation cell to obtain the correct free volume. We have tried three geometries, all of which yielded essentially the same results. In all cases, we monitored the potential energy and spacing of atoms in the crystals to detect the presence of a uniaxial strain. In two calculations, the y borders were periodic and in the third they were free surfaces. Although we finally decided on a 56-atom cell for the dynamic simulation, cells with up to 84 atoms ($YL = 42$ [010] DSC) were investigated. The most definitive results were obtained on the 84-atom cell with free y borders, but the results of the other calculations also have some interesting aspects.

The static relaxations were carried out by two different simulation techniques, both giving essentially the same results. In the molecular dynamics technique the atoms moved under the influence of mutual interactions, but as the system evolved in time, a small damping was applied so that the system gradually cooled down and the atoms settled into a configuration of zero net force.[13] Another technique used to obtain a force-free configuration was a conjugate gradient method.[18]

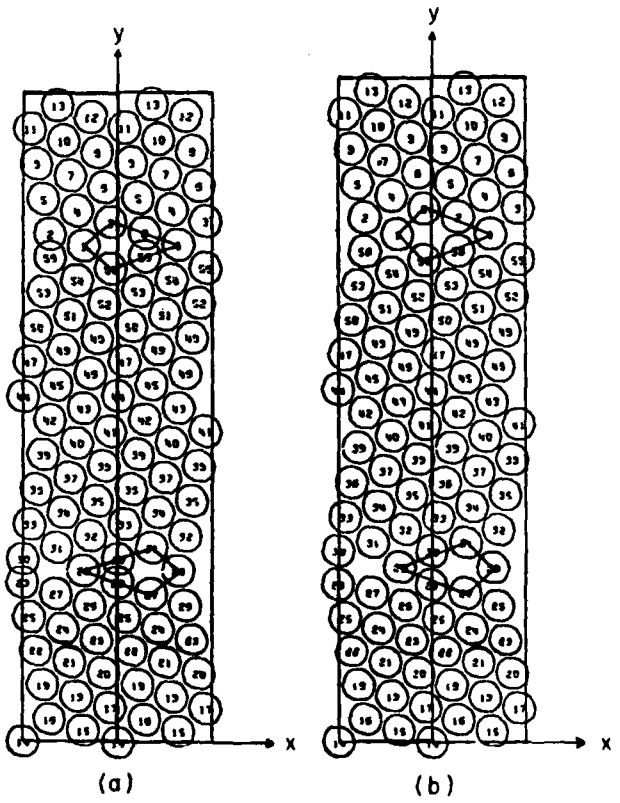

FIG. 2. Cell of 56 atoms used in the present computer molecular dynamics simulation of grain boundary migration. (a) Initial unrelaxed configuration showing the close overlap of atoms 2 and 56, and 29 and 30. (b) Configuration prior to dynamic simulation—fully relaxed including relief of longitudinal compression by slight increase of cell dimension along the y direction.

In the calculations with periodic y borders at $YL = 28$ [010] DSC, the 56-atom cell shown in Fig. 2(a) was relaxed without any changes of the border positions. Upon relaxation a uniaxial compressive strain developed. In order to remove this strain, we increased YL in small steps and repeated the relaxation each time. This procedure led to a minimum in potential energy of the cell at $YL = 28.6085$ [010] DSC, and an average y separation of 0.5 [010] DSC for the {541} planes midway between the boundary (the perfect crystal value) at almost this same value, $YL = 28.6070$ [010] DSC. The relaxed structure corresponding to the latter YL value is shown in Fig. 2(b). This structure is simply the initial structure expanded in the y direction by 0.304 [010] DSC per boundary, i.e., giving $V_f = 0.304$ atomic volume per period. Several authors have stressed the importance of permitting global rigid-body translations of one crystal with respect to the other in a direction parallel to the boundary (x here) as a relaxation adjustment.[19] The present relaxed structure for the boundary system with the Lennard-Jones potentials did not result in any x translation, in spite of the fact that such translations were consistent with the use of periodic borders as shown by the calculations to be described next.

In a second calculation using periodic y borders, we removed one of the atoms in the tight pair in each boundary period. This created a 54-atom cell with $YL = 28$ [010] DSC, the initial length of the 56-atom cell. The effect of a series of individual atomic relaxations was that one crystal underwent a global translation in the x direction, with respect to the other, and the atoms near the boundary relaxed in toward the boundary leaving a tensile strain in the center of the crystal. Subsequent adjustment of the y dimension to relieve this tensile strain yielded the *same relaxed configuration* as above with the same value of V_f but in a shorter computational cell corresponding to the reduced number of atoms. This calculation demonstrated rather dramatically that periodic borders do not inhibit global translations, and that the structure in Fig. 2(a) arrived from quite different paths was very likely the minimum energy structure. It also shows that the *structural vacancy* arises naturally from the relaxation procedure rather than from an arbitrary initialization.

In both the 54- and 56-atom cells, adjustments of YL were used to obtain a region in the center of the crystals which on the average had no uniaxial strain. However, we could not eliminate a slight strain gradient indicating that the elastic fields of the boundaries were overlapping slightly. To explore this we increased the cell size to 84 atoms, with $YL = 42$ [010] DSC, and used free surfaces as y borders. This left the atoms in the cell quite free to move outward so that the proper free volume was obtained quite naturally. After the relaxation this cell had a region 7 [010] DSC in length in which the potential energy of individual atoms was within 1 part in 10^6 of the values obtained in the other calculations, and the interplanar spacing of the {541} planes was within 1

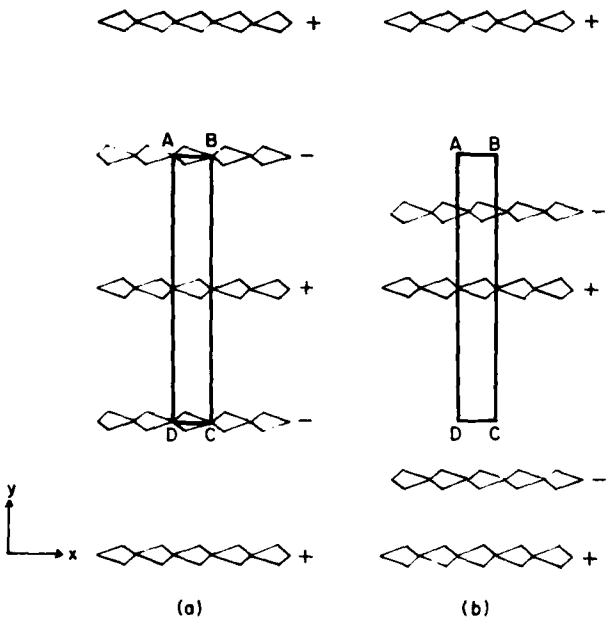

FIG. 3. (a) The initial microstructure produced by periodic extension in the x and y directions of the computational cell ABCD. (b) The microstructure after one boundary, indicated by the minus sign, has migrated downward.

part in 10^4 of the perfect crystal values. To the same degree of resolution the strain field of the free surface extended inward by 4.5 [010] DSC, and that of the boundary outward by 9.5 [010] DSC. V_f was again 0.340 atomic volume period. The extent of the boundary strain field in units of the boundary period was 2.4. This is comparable to what we found in relaxing a $\Sigma = 5\{310\}$ twin boundary in three-dimensional simulations of a boundary in a fcc crystal with Lennard-Jones potential.[20]

It might naively have been expected that a grain boundary would perturb the crystal away from it over a smaller distance than would a free surface. The present results to the contrary suggest a perhaps equally naive explanation that because the free surface is unconstrained, local relaxation can take place to a greater degree than in the grain boundary without requiring as strong a perturbation below the surface.

The above results show that in the 56-atom cell used in the molecular dynamics simulations the boundaries perturb each other through their elastic fields. Initially the microstructure generated by the periodic extension of the cell in the x and y directions consists of an array of equally spaced boundaries [Fig. 3(a)]. When the symmetry is broken by thermal fluctuations, a pair of boundaries may migrate together with continuous attraction, continually "consuming" the crystalline region in between, until they finally annihilate each other leaving in the system a single crystal. In the molecular dynamics simulation on the 56-atom cell, this process was actually observed at sufficiently high temperatures.

It should be noted that as a final check on our static relaxation, we ran the molecular dynamics program without any damping force and assigned all the particles zero initial velocity. If the system were not in a relaxed configuration the particles would experience a net force and therefore would move. With the configuration shown in Fig. 2(b) the particles remained essentially motionless for several hundred time steps of simulation.

III. THRESHOLD FOR GRAIN-BOUNDARY SLIDING

In any consideration of the dynamics of grain boundaries, sliding is one of the basic modes of motion.[21–23] When viewed in terms of atomic displacements this is a highly cooperative process since it involves the translation of one group of particles relative to another group. To identify such processes in our simulation we have adopted the following convention which seems reasonable to us but is admittedly arbitrary. Since instantaneous atomic displacements have a component associated with thermal vibrations present in any finite-temperature simulation, we consider only displacements that have been averaged over 100 time steps, an interval that is several times the typical vibrational periods. With this averaging we expect that much of the short-time vibrational effects are eliminated. Futhermore, we will regard sliding to have occurred when the relative displacement of one group of atoms relative to another is equal to or greater than one DSC unit along the x direction.

Figure 4 shows a typical pattern of average particle displacements in the x direction during a relatively early stage of a simulation. One can see that particles numbered 1 through 25 all have positive displacements. This configuration, which indicates that boundary sliding has occurred, developed after the system was allowed to come to equilibrium at a particular temperature. Boundary sliding, however, did not always occur whatever the temperature; in fact, for a given length of simulation there was a temperature below which sliding was not observed.

Since all simulations began with a relaxed configuration, the energy necessary to activate the sliding process must come from the thermal energy of the particles. While it is difficult to define and determine precisely the potential energy barrier to sliding, we have established a correlation

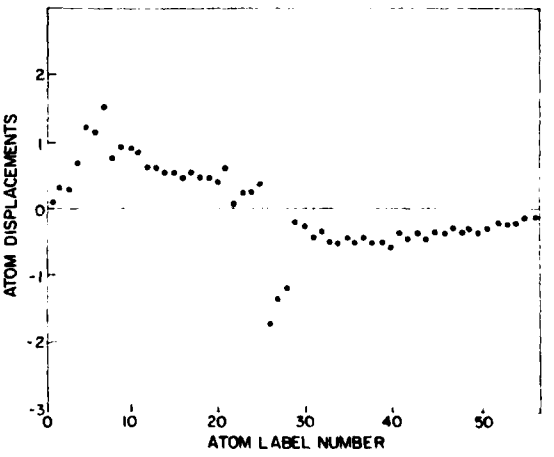

FIG. 4. Atomic displacements along the x direction (in units of XDSC). The displacements are averaged values over an interval of 100 time steps and are taken during a relatively early stage of the simulation.

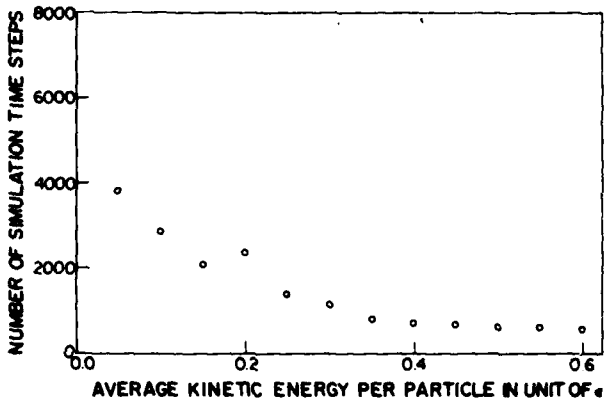

FIG. 5. Variation of "waiting time" (in units of simulation time steps) prior to the onset of boundary sliding as a function of the average kinetic energy per particle (in unit of ϵ, the well depth of the Lennard-Jones potential function).

between the average kinetic energy per particle and the time at which sliding commences. Figure 5 shows that at lower system temperatures the waiting time for sliding increases. This behavior is quite reasonable since the activation energy is provided by thermal fluctuations and the necessary fluctuations should occur less frequently at lower temperatures. As also shown in Fig. 5, at sufficiently high temperatures the time at which sliding occurs appears to be insensitive to temperature, thus indicating that even when there is sufficient thermal energy to overcome the barrier the system requires a certain period of time for equilibration, perhaps dependent on dynamical processes. At an average kinetic energy per particle of 0.025ϵ sliding was not observed in a simulation run extending out to 15 000 time steps. We regard this as evidence that the sliding processes observed here are thermally activated. In such thermally activated processes a threshold temperature exists below which the probability of sliding within a given time interval decreases exponentially.

IV. COUPLED BOUNDARY SLIDING AND MIGRATION

A competing process to boundary sliding is boundary migration.[21,22] This process involves the motion of the grain boundary in the y direction in our simulation cell. Our simulation results showed that both migration and sliding processes could take place, and the general movements of a grain boundary can be described as sequences of *coupled* sliding and migration. It is possible to follow the detailed sequence of atomic motions which occur during migration. These motions involve the correlated sequential motion of a number of atoms. Two different sequences have been observed in which the boundary moves either three or four {541} planes during the migration sequence. As will be discussed in more detail later, the migration sequences also involve a localized shearing or sliding of one crystal with respect to the other. The sequences are in fact those of migration-sliding.

By following a group of atoms (two groups are indicated in heavy circles), one can readily discern how the structure changes in the process. In the initial configuration, Fig. 6(a), a kite-shaped group shows the boundary plane is at atom 1 and a ring of atoms surrounds atom 3 which is part of the upper bicrystal. At the end of the sequence, Fig. 6(c), the boundary has moved to atom 4, a migration of three {541} planes, while atom 3 is now clearly part of lower bicrystal. Figure 6(b) shows a saddlepoint or activated state configuration with atom 3 in the middle of the ring.

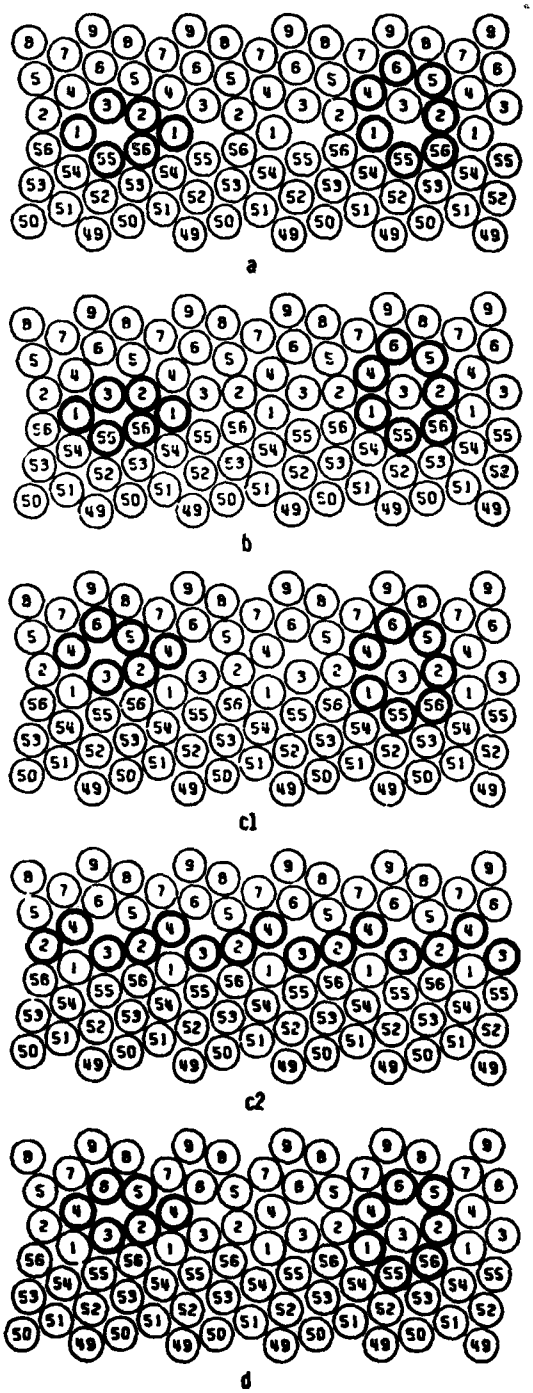

FIG. 6. Sequence of upper grain boundary configuration as in Fig. 2(b) showing coupled sliding and migration. Each configuration, except that of $t = 0$, is an average over an interval of 100 time steps starting at time step, t. (a) $t = 0$, (b) $t = 1401$, (c) $t = 1501$, (d) $t = 1701$.

Comparing the vertical alignment of atom pairs (2,5) and (4,1) at the beginning and the end of the sequence, one can detect a sliding, or shearing, of the upper bicrystal to the right. Thus in the same sequence sliding and migration have both occurred. Notice that atom 6 was lined up initially with atom 52, and at the end of the sequence it was lined up with atom 55. The amount of sliding is [100] DSC by referring to the positions of atom 52 and 55 in Fig. 1.

We have also observed and carried out a similar analysis of migration-sliding sequence involving the boundary traversing four {541} layers (2 [010] DSC). The activated state is the same, but the relative shear is different.

V. GRAIN-BOUNDARY ANNIHILATION

The two grain boundaries in the simulation cell are coupled through the strain field and through the thermal vibrations. If the boundaries move toward each other sufficiently, they can combine to form a perfect crystal. We will call this process "boundary annihilation." One can calculate the potential energy of the system with two boundaries in its relaxed configuration, as shown in Fig. 2(b), and the potential energy of a perfect crystal specimen with the same number of particles and the same area. This difference in potential energy contributes to the activation energy for boundary annihilation. However, boundary annihilation will not occur spontaneously at zero temperature since sliding and migration processes require thermal activations.

We have observed boundary annihilation in our simulations. The annihilation process is apparently quite complicated, and it did not occur immediately after the commencement of sliding and migration. The picture which emerged from our results is that at a given temperature above the threshold the system requires a certain average time interval, which we may call "incubation period," to initiate the sliding and migration processes. Then there follows a time interval during which the boundaries move in a stochastic manner. Finally the two grain boundaries steadily move toward each other and annihilate.

The post annihilation, single crystal structure is shown in Fig. 7(c). From this result and the initial configuration, Fig. 7(a), with two grain boundaries one obtains a typical displacement field giving the net atomic displacements. Subtracting the atomic positions in the initial configuration one obtains the indicated net displacement field. From this, one can infer that the boundaries did not migrate through the central region of the simulation cell on their way to annihilation. Details of the displacement field clearly depend on the particular sequence of sliding and migration processes involved, and different field patterns have been obtained in simulation runs using different sets of random numbers for initialization.

It is instructive to examine the annihilation process from the standpoint of the excess thermodynamic functions per unit area of the grain boundary. The excess energy arises from the different *average configuration* of the boundary atoms with respect to those in the crystal, as well as the differences between the contribution to potential energy arising from the temperature-dependent position fluctuations. This latter contribution results from the different anharmonic vibrational energies of the boundary atoms from those of atoms in the perfect lattice. There is also an excess entropy arising from corresponding differences in harmonic and anharmonic vibrational entropies between the grain-boundary and the perfect-lattice systems. Finally, there may be a $P\Delta V$ contribution to the excess enthalpy or Gibbs free energy arising from the excess boundary volume. The annihilation process was observed to produce an increase of average temperature, or equivalently the average kinetic energy per particle, as shown in Fig. 8. Annihilation occurred in this case at about time step 3600.

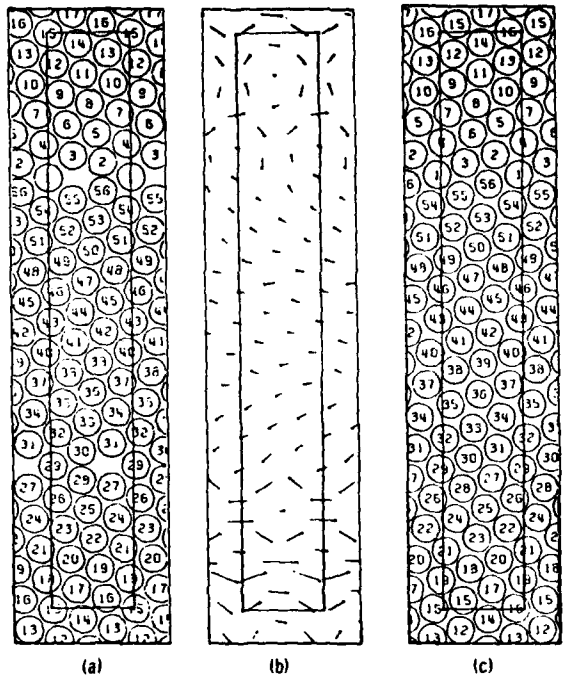

FIG. 7. Simulation cell showing the actual net motions of the atoms associated with the migration of the two grain boundaries from initial configuration (a) to annihilation. The total net displacements (magnified by a factor of 2) of the atoms are given in (b), while (c) represents the atomic configuration averaged over 100 time steps after annihilation.

VI. EXCESS FREE AREA AND STRAIN DISTRIBUTION

We have thus far considered the dynamics of grain boundaries in terms of individual particle motions. Another way of discussing the simulation results is to analyze the *distribution* of *excess free area* in the system at various stages of dynamical evolution. Our simulation cell contains a total excess free area equal to 1.22 ($V_f = 0.304$, two boundaries and two periods) times the area occupied by an atom in the perfect crystal when we compare the cell area of the boundary system to that of the corresponding perfect crystal. Most of this excess is initially localized in the immediate region of the two grain boundaries, but as the boundaries begin to slide and migrate, the free-area distribution can also change.

To determine the distribution of free area under dynamical conditions, we have adopted the procedure of Argon and Kuo[24] for estimating the excess free area in a local

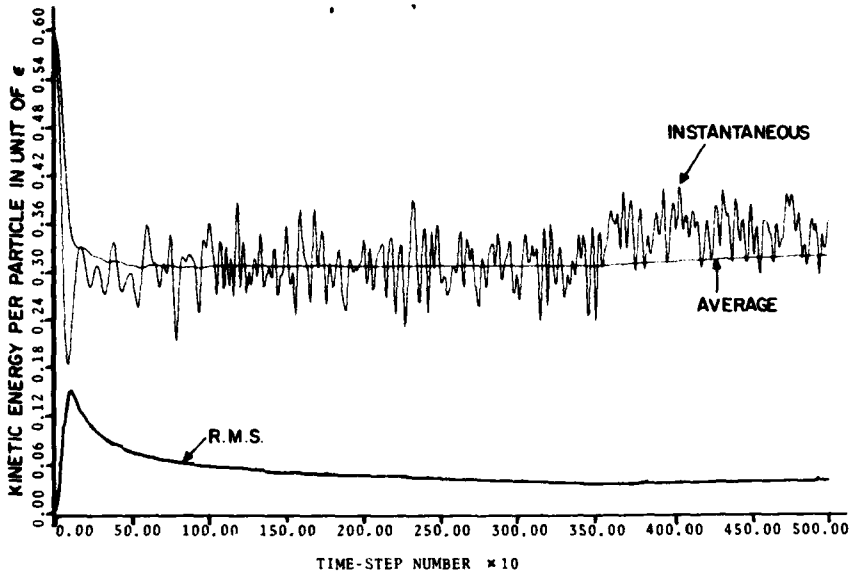

FIG. 8. Instantaneous and time-averaged kinetic energy per particle (in unit of potential well depth ϵ). One can observe an increase in kinetic energy after time step 3600 as a result of boundary annihilation. Also shown is the root mean-square deviation.

region (Fig. 9). While the excess free area thus defined is not always entirely concentrated in the grain-boundary regions, *movements* of the excess free area indeed follow the motions of the boundaries.[25] When the boundaries annihilate at approximately time step 3600, the excess free area cannot vanish because the simulation is carried out at constant area. Moreover, it appears that the excess free area is not redistributed uniformly throughout the cell; rather, it remains localized though not static. It is possible that the free areas can *coalesce* and form a vacancy, although we have not observed this process in any of our simulations.

In an attempt to display the deformations that occur during sliding and migration, we have carried out an analysis of the local shear and dilation strains using a procedure[24] that makes use of particle positions at two successive time steps. The results are shown in Fig. 10, where the strains

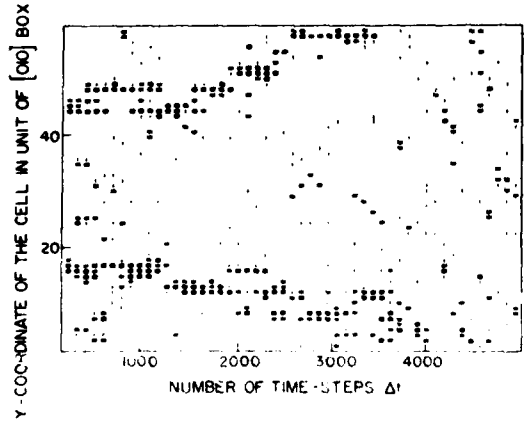

FIG. 9. Distribution of excess free area in the simulation cell under dynamic conditions. The cell is divided into 540 boxes with 60 along the y direction. At a fixed y coordinate, only the box with the largest free area is considered, and a symbol is shown for that y coordinate if this free area exceeds the average free area value in the corresponding perfect crystal cell. Three symbols are used to indicate relative magnitudes: •, ∗, and 1 in increasing order of excess free area.

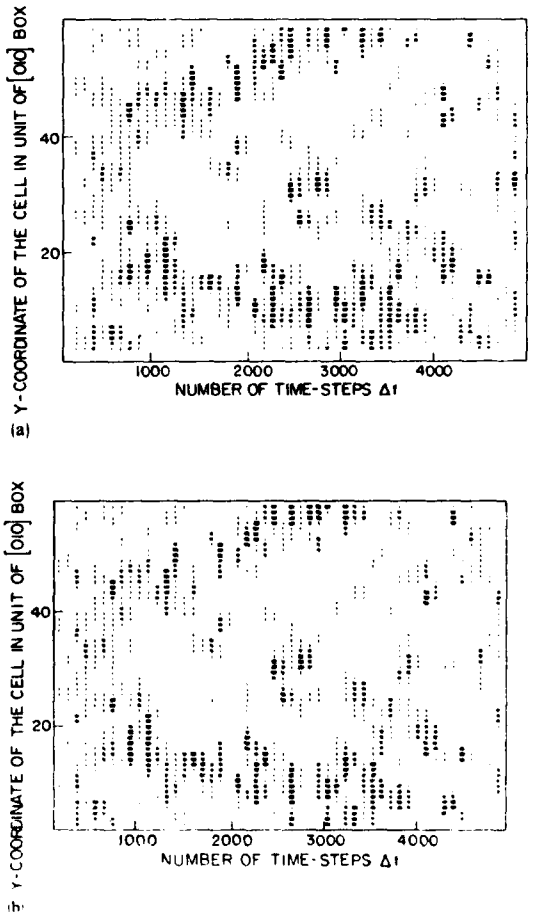

FIG. 10. Strain distribution in the simulation cell under dynamic conditions. The cell is divided into 540 boxes with 60 along the y direction. At a fixed y coordinate, only the box with the largest strain is considered, and a symbol is shown for the y coordinate if the strain exceeds the average strain in the corresponding perfect crystal cell. Three symbols are used to indicate relative magnitudes: •, ∗, and 1, in decreasing values of strain. (a) Dilation strain, (b) shear strain.

have been averaged over 100 time steps and different symbols are used to indicate relative magnitudes as was done in Fig. 9. Both shear and dilation strains are seen to be higher in the grain-boundary regions, as we would expect. When there was no boundary migration, their magnitudes were relatively small. During migration high strains were developed in the boundary region, indicating that when atoms have to slide relative to each other they also induce considerable deformations in the perpendicular direction.

In Fig. 10 one can see that although the system was initially strain free, both shear and dilation strains quickly built up after the start of the simulation, and they moved through the cell following the grain boundaries. Also, the strains were not concentrated only in the boundary regions. For example, around time steps 2500–3000, there appeared a region of shear and dilation strains in the center of the cell while the two boundaries were actually located at the top and bottom edges of the cell. After annihilation there was considerable residual strain in both shear and dilation. These, however, were not distributed in any localized manner.

ACKNOWLEDGMENTS

The work of T. Kowk and S. Yip has been supported by Army Research Office Contract No. DAAG-29-78-C-0006. We also gratefully acknowledge discussions with Professor A. A. Argon and Dr. H. Y. Kuo on the strain calculation.

[1]See, for example, *Grain Boundary Structure and Properties*, edited by G A. Chadwick and D. A. Smith (Academic, New York, 1976).
[2]*Interatomic Potentials and Simulation of Lattice Defects*, edited by P. C. Gehlen, J. R. Beeler, and R. I. Jaffee (Plenum New York, 1972).
[3]J. R. Beeler, in *Advances in Materials Research*, edited by H. Herman (Wiley, New York, 1970), Vol. 4, p. 295.
[4]*Computer Simulations for Materials Applications* Nuclear Metallurgy, Vol. 20, Parts 1 and 2 edited by R. J. Arsenault, J. R. Beeler, and J. A. Simmons (National Bureau of Standards, Washington, D. C., 1976).
[5]C. H. Bennett, in *Diffusion in Solids: Recent Developments*, edited by J. J. Burton and A. S. Nowick (Academic, New York, 1975), p. 73.
[6]There exists now an extensive literature on computer molecular dynamics and Monte Carlo simulations and various applications. For a bibliography, see W. Wood and J. J. Erpenbeck, Ann. Rev. Phys. Chem. **27**, 319 (1976).
[7]See the review of R. J. Harrison, G. A. Bruggeman, and G. H. Bishop, in *Grain Boundary Structure and Properties*, edited by G. A. Chadwick and D. A. Smith (Academic, London, 1976), p. 45.
[8]R. M. J. Cotterill, T. Leffers, and H. Lilholt, Philos. Mag. **30**, 265 (1974).
[9]G. H. Bishop, G. A. Bruggeman, R. J. Harrison, J. A. Cox, and S. Yip, in Ref. 4, p. 522.
[10]G. H. Bishop, R. J. Harrison, T. Kwok, and S. Yip, Trans. Am. Nucl. Soc. **27**, 323 (1977). Some of the observations have been discussed along with three-dimensional simulation results in Ref. 11.
[11]G. H. Bishop, R. J. Harrison, T. Kwok, and S. Yip, in *Progress in Materials Science, Chalmers Anniversary Volume*, edited by J. W. Christian, P. Haasen, and T. B. Massalski (Pergamon, Oxford, 1981), p. 49.
[12]W. Bollman, *Crystal Defects and Crystal Interfaces* (Springer, New York, 1970).
[13]T. Kwok, M. S. thesis, Dept. of Nuclear Engineering, MIT (1978).
[14]M. L. Kronberg and F. H. Wilson, Trans. AIME **185**, 501 (1949).
[15]D. H. Smith and R. C. Pond, Metall. Rev. **205**, 61 (1976).
[16]G. H. Bishop and B. Chalmers, Philos. Mag. **24**, 515 (1971).
[17]Free area might be a better term in a two-dimensional simulation, but we shall use the more general term free volume, except in a later section where we specifically measure free area.
[18]J. E. Sinclair, and R. Fletcher, J. Phys. C **7**, 864 (1974).
[19]R. C. Pond and D. A. Smith, Can. Metall. Q. **13**, 39 (1974); R. C. Pond, D. A. Smith, and W. A. T. Clark, J. Microsc. **102**, 309 (1974); R. C. Pond and V. Vitek, Proc. R. Soc. London B **357**, 453 (1977); P. H. Pumphrey, T. F. Mailis, and H. Gleiter, Philos. Mag. **34**, 227 (1976).
[20]G. H. Bishop, R. J. Harrison, T. Kwok, and S. Yip, J. Appl. Phys. **53** 5596(1982).
[21]M. F. Ashby, Surf. Sci. **31**, 498 (1972).
[22]R. N. Stevens, Metal. Rev. **2**, 129 (1966).
[23]G. A. Bruggeman, G. H. Bishop, J. A. Cox, and R. J. Harrison, in Ref. 4, p. 450.
[24]A. S. Argon and H. Y. Kuo, Mater Sci. Eng. **39**, 101 (1979).
[25]Our simulation cell is such that if we divide the cell area into 60 squares, 3 along the x direction and 20 along the y direction, there will be roughly one particle per square. To obtain some spatial resolution we then divide the cell into 540 boxes, 9 along the x direction and 60 along the y direction In addition, each box is further divided into 25 small boxes, 5 along each direction. At any given time the small boxes which contain the atom centers are found, these boxes and the 224 nearest boxes surrounding each one are considered to be occupied (overlap is allowed). By counting the number of unoccupied small boxes in each large box we determine the free area in that large box. We then repeat the same procedure for the perfect crystal. By excess free are we mean those cases where the number of unoccupied small boxes exceeds the maximum number of unoccupied small boxes found in the perfect crystal. These cases are then divided into three groups with each indicated by a different symbol in Fig. 12.